INL/CON-22-66403-Revision-0

Overview of Base Model in Parametric Studies Specific to Performance of U-Mo Plates

October 2022

Hakan Ozaltun, Hee Seok Roh, Walid Mohamed

Changing the World's Energy Future

INL is a U.S. Department of Energy National Laboratory operated by Battelle Energy Alliance, LLC

INL/CON-22-66403-Revision-0

Overview of Base Model in Parametric Studies Specific to Performance of U-Mo Plates

Hakan Ozaltun, Hee Seok Roh, Walid Mohamed

October 2022

Idaho National Laboratory
Idaho Falls, Idaho 83415

http://www.inl.gov

Prepared for the
U.S. Department of Energy
Under DOE Idaho Operations Office
Contract DE-AC07-05ID14517

Proceedings of the ASME 2022
International Mechanical Engineering Congress and Exposition
IMECE2022
October 30 - November 03, 2022, Columbus, Ohio

IMECE2022- 93718

OVERVIEW OF THE BASE MODEL FOR THE PARAMETRIC SENSITIVITY STUDIES SPECIFIC TO PERFORMANCE ASSESSMENTS OF U-MO FUEL PLATES

Hakan Ozaltun[1]
Idaho National Laboratory
Idaho Falls, ID, USA

Hee Seok Roh
Argonne National Laboratory
Lemont, IL, USA

Walid Mohamed
Argonne National Laboratory
Lemont, IL, USA

ABSTRACT

This paper provides an overview of the base model specifically developed to perform parametric sensitivity studies on the U-10Mo monolithic fuel system. U-Mo monolithic fuels are being considered for the conversion of test reactors into high-performance research reactors that operate using proliferation-resistant, low-enriched uranium (LEU) fuels. These plate-type fuels contain a high-density, low-enrichment fuel sandwiched between zirconium diffusion barriers and encapsulated in aluminum claddings. All U.S. high-performance research reactors have released the designs of their LEU monolithic fuel reactor cores. These designs include nearly 50 distinct fuel plate geometries with different operational parameters. Consequently, a single generic plate geometry representing all the extreme points in this design matrix is unrealistic. To evaluate the performance for various parameters, a set of sensitivity studies was performed. These studies considered various input parameters (i.e., geometric, operational, and material property-related). The results revealed valuable information about plate performance and the sensitivity of this performance to various modeling inputs. To establish a reference state for comparing these result, base model featuring representative irradiation conditions was developed. To capture in-reactor behavior accurately, incorporation of representative constitutive models capable of evolving properties with respect to temperature, irradiation time, and burnup was needed. The behavioral models considered burnup-dependent properties, swelling, creep, and degradation. This paper introduces the base model created for the parametric sensitivity studies. The detailed description of the procedure includes the model geometry, model discretization, thermo-mechanical coupling, material properties and behavioral models. This paper also provides selected results and assesses the performance of the base model.

1. INTRODUCTION

The goal of the Material Management and Minimization Reactor Conversion Program is to develop technologies for converting test reactors into reactors that operate using proliferation-resistant, low-enriched uranium (LEU) fuels. As part of this goal, the U.S. High-Performance Research Reactor Fuel Qualification Program has been evaluating the performance of a U-10Mo-alloy-based monolithic plate-type fuel system. The program is now moving into the qualification phase, anticipating the timely conversion of the target reactors. To qualify this fuel system, the program must demonstrate that the system meets all safety standards and performs well in the reactor environment. The requirement of maintained mechanical integrity and structural stability under normal operating conditions is primarily demonstrated via successful testing at up to the limiting conditions defined by the fuel performance envelope, including adequate margin of safety.

All high-performance research reactors have released the designs of their LEU monolithic fuel reactor cores. While these designs may require modifications, they are sufficiently mature to be considered in fabrication development efforts. These unique plate designs necessitate nearly 50 distinct LEU fuel plate geometries with different operational parameters.

A single generic plate geometry featuring pre-defined irradiation specifics representing all the extreme points in this design matrix is unrealistic, since the two extremes of a given parameter would yield entirely different performance evaluations. Consequently, it is infeasible to use in-reactor testing to evaluate the performance of plates featuring a large set of geometric design variables with different operational parameters. In the absence of such experimental evaluations, simulations can serve as a timely

[1] Contact author: hakan.ozaltun@inl.gov, (208) 526-0274

and cost-effective means of evaluating the in-reactor behavior of plates with varied types of parameters, including plate design, material properties, geometric irregularities, and operational conditions. The simulations also serve as an integration function, in which individual fuel performance phenomena are combined and evaluated in the context of complex irradiation environments. Fuel performance modeling also provides valuable input for establishing manufacturing defect limitations, provides useful information for interpretating characterization and post-irradiation examination results, and enables assessment of various phenomena such as geometric changes and failure mechanisms. Responses to specific operating or upset conditions can also be evaluated.

To support the qualification efforts, a comprehensive parametric sensitivity study campaign was specifically launched to explore the irradiation performance of the plates, and to evaluate the sensitivity of this performance to various input variables, including (1) geometric parameters, (2) operational parameters, and (3) material-property-related parameters.

This paper introduces the base model used in those parametric sensitivity studies. The detailed description of this model includes the geometric features, model discretization, thermal and structural coupling, material properties, and modeling considerations. This paper also provides selected results from the simulations applied to the assessment of thermo-mechanical performance.

2. BASE MODEL

To establish a reference state for the parametric sensitivity studies, a base model featuring a representative geometry and irradiation conditions was created. The following sections discuss the plate geometry, irradiation parameters, and material properties used to build the base model.

2.1 Geometry of the base model

The geometric dimensions were based on the specifications defined for plates used in the MP-1 experimental campaigns. The MP-1 experiments featured plates with two different fuel thicknesses. Based on the dimension of the plates for "thin fuel," the fuel in this work was modeled as being 82.550 mm long, 19.050 mm wide, and 0.216 mm thick. The plate dimensions were taken to be 101.473 mm long, 25.400 mm wide, and 1.245 mm thick. The diffusion barrier was modeled as being 0.0254 mm thick over the fuel zone. This geometric configuration is shown in FIGURE 1.

2.2 Discretization of the model

In the base model, the fuel thickness was represented by six layers, the cladding thickness by five, and the diffusion barrier thickness by three, for a total of 22 layers through the thickness of the plate. The nodal divisions in the length and width directions of the plate were 210 and 52, respectively. This discretization scheme resulted in 240,240 hexahedral elements.

The C3D8RT element of ABAQUS [1], an 8-node thermally coupled brick, and tri-linear displacement and temperature with reduced integration and hourglass control were used. A mesh sensitivity study was carried out to minimize the computational time. The results of the sensitivity study indicated that a further increase in the number of layers through the thickness of the plate would not change the results, as has been explained elsewhere [2]. Therefore, total 22 through thickness layers were utilized.

This discretization scheme and mesh density remained unchanged in all the subsequent sensitivity studies to avoid any effects potentially introduced by employing a coarser or finer mesh in the simulations.

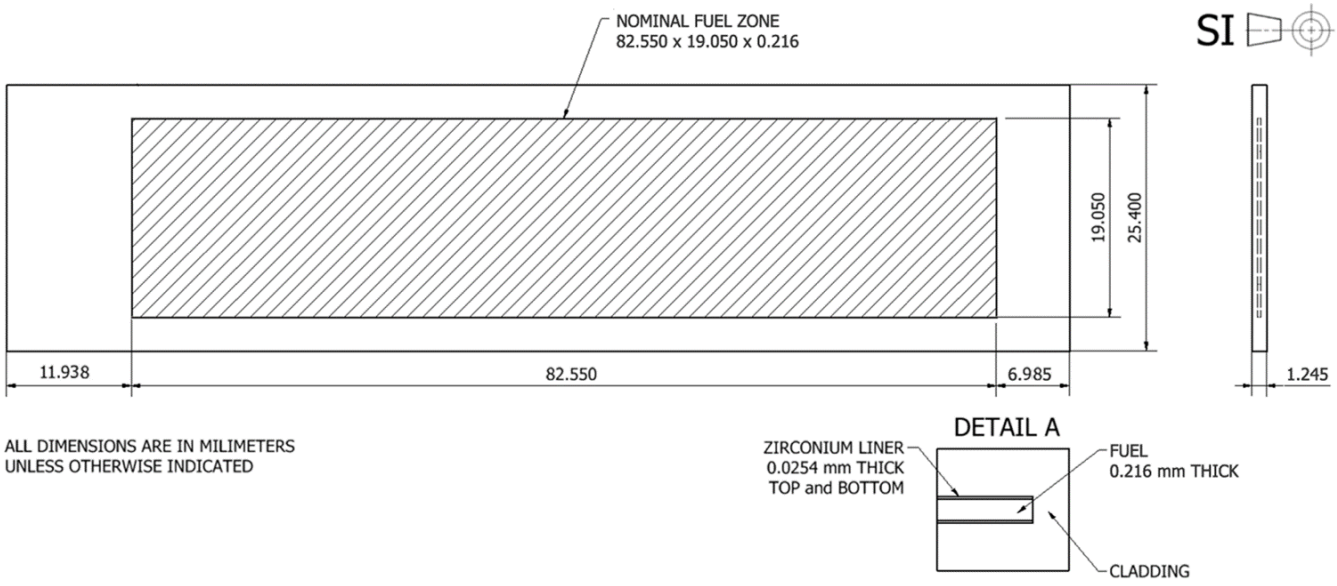

FIGURE 1: PLATE DIMENSIONS (MM) OF THE BASE MODEL USED IN PARAMETRIC SENSITIVITY STUDIES

2.3 Irradiation parameters for the base model

Irradiation conditions were also taken from the MP-1 experiments. The base model was irradiated over a single continuous cycle that lasted for 53 days (1,272 hours).

For a conservative evaluation, the plates were evaluated at high power and high burnup. The fission power density was taken to be 32,776 W/cm^3, and the average fission density was taken to be 7.7E+21 (fissions/cm^3), aiming for near-total burnup at end of life (EOL). The fast neutron flux (>0.1 MeV) was taken to be a constant 2.220E+14 n/cm^2-sec throughout the irradiation process, resulting in a fast fluence of 1.017E+18 n/cm^2 at EOL.

The experimental plates are irradiated in either edge-on or face-on configurations at the Advanced Test Reactor (ATR). Such orientations naturally create a non-uniform fission profile distribution in the fuel zone, leading to non-linearities. In the base model, however, the fission profile (local-to-average ratio) was incorporated as being constant to avoid creating any artificial effects. The irradiation parameters are in FIGURE 2.

2.4 Modeling considerations

The bonding between the foil, cladding, and diffusion barrier was assumed to be ideal, with no defects prior to irradiation. It was also assumed that no interfacial delamination occurs during the irradiation process. Therefore, all nodal points at the interfaces were tied together. The plate was modeled as being free to move in all directions except along its longitudinal edges. At the one longitudinal edge, only the sliding motion was permitted. Opposite longitudinal edge was permitted to displace in length and width direction only, as these edges are constrained by the rails of the capsule. One single node on the cladding corner was fixed to prevent rigid body motion.

A fully coupled thermal-displacement transient solver with active swelling-creep-viscoelastic behavior was used. An explicit-implicit integration scheme was used. The maximum time increment per step was set at 24 hours, and the maximum temperature change per step was set at 10°C to avoid instabilities

The models featured fully coupled thermal-structural interactions with user-defined parameters. For the base model, a fully coupled 3-D model of a monolithic plate was created, capable of evolving the thermo-mechanical properties with irradiation time and burnup. The models used the plate geometry, irradiation history, and coolant conditions as input.

Irradiation-specific parameters were incorporated by several user-defined routines. Fission density and neutron flux with respect to the spatial coordinates and irradiation time were introduced into the USDFLD subroutine of ABAQUS [1]. Cladding and diffusion barrier properties, including radiation hardening and growth, were varied as a function of fast neutron exposure. Degradation models for the fuel were implemented as a function of fission density. Irradiation creep and swelling of the fuel, due to solid and gaseous products, were implemented by the subroutine CREEP.

2.5 Material properties and behavioral models

Behavioral modeling of fuel plates involves the integration of several tightly coupled phenomena. This multi-physics coupling inherently necessitates consideration of many parameters to assess overall fuel performance. Stresses, strains, deformations, and temperatures are generally evaluated together to provide an accurate performance assessment of the fuel plate throughout its service life.

For the base model used in the sensitivity studies, the incorporation of representative constitutive models capable of evolving properties with respect to temperature, irradiation time, and burnup was needed. These behavioral models included burnup-dependent properties, fission product swelling, irradiation creep, and relevant property degradation models.

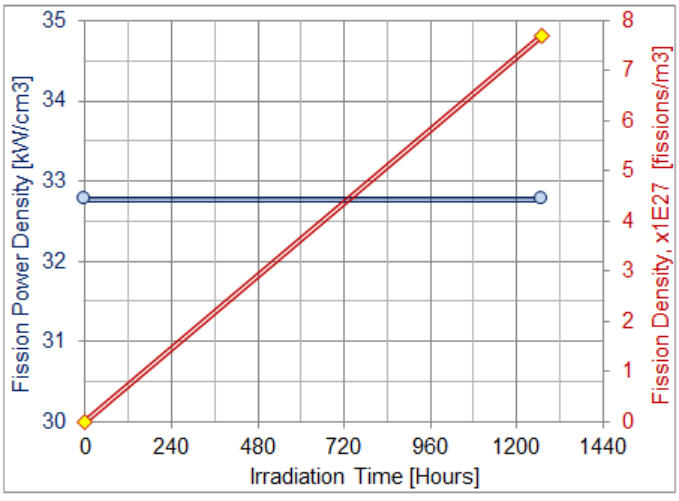

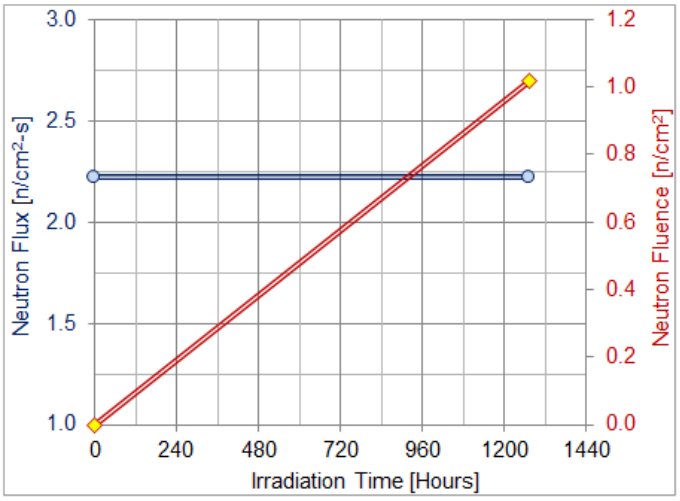

FIGURE 2: **(A)** HEAT GENERATION RATE AND FISSION DENSITY **(B)** FAST NEUTRON FLUX AND FLUENCE (>0.1 MEV) AT EOL

2.5.1 Fuel behavioral models

The fuel material used in this study was monolithic U-10Mo. The thermo-mechanical models of the fuel were based on temperature- and burnup-dependent data.

Behavioral models for the fuel core included elasticity, plasticity, thermal expansion, irradiation creep, volumetric swelling, modulus degradation, and thermal conductivity degradation due to porosity increase.

The model for fuel swelling due to fission products was based on the relation given by Robinson [3]:

$$\%\left(\frac{\Delta V}{V_0}\right)_f = 6.13 \times 10^{-43} f_d^2 + 4.00 \times 10^{-21} f_d \quad (1)$$

where $\%\left(\frac{\Delta V}{V_0}\right)_f$ is the total percent swelling of the fuel core and f_d is the fission density in fissions/cm^3.

Solid swelling was based on a model proposed by Kim [4]

$$\%\left(\frac{\Delta V}{V_0}\right)_s = 4.00 \times f_d \quad (2)$$

where $\%\left(\frac{\Delta V}{V_0}\right)_s$ is the total percent swelling of the fuel core, due to solid fission products, and f_d is the fission density in $\times 10^{21}$ fissions/cm^3.

Gaseous swelling was estimated by subtracting the solid swelling from the total swelling:

$$\%\left(\frac{\Delta V}{V_0}\right)_g = 6.13 \times 10^{-43} f_d^2 \quad (3)$$

where $\left(\frac{\Delta V}{V_0}\right)_g$ is the gaseous swelling in (%) and f_d is the fission density in fissions/cm^3.

The irradiation creep model was based on a correlation proposed by Kim [5]:

$$\dot{\epsilon} = A \cdot \sigma \cdot \dot{f} \quad (4)$$

where $\dot{\epsilon}$ is the creep strain rate (1/sec), A is the irradiation- creep rate coefficient (500×10^{-25} cm^3/MPa), σ is the equivalent stress (MPa), and $\dot{f}$ is the fission density rate (fissions/cm^3-sec).

The modulus of elasticity of unirradiated fuel as a function of temperature was created from data reported by Schulthess [6]:

$$E = 91.2 - 0.140 \times T \quad (5)$$

where E is the modulus in GPa, and T is the temperature in °C. The relation is valid for 20–550°C.

Given the difficulty of the measurements, the limited data available, and the relatively large uncertainties, a linear fit trend representing the degradation of the fuel elasticity modulus was developed using data provided by Schulthess [7]:

$$E = 85 - 6.8 \times FD \quad (6)$$

where E is the elasticity modulus of irradiated U-10Mo at room temperature in GPa, and FD is the fission density in 10^{21} fissions/cm^3. The relation is valid at up to ~6×10^{21} fissions/cm^3.

For modeling purposes, the modulus of irradiated fuel at elevated temperatures was needed to capture the fuel behavior. Because irradiated property data were only available at room temperature, the unirradiated model in Equation 5 and the irradiated model in Equation 6 were evaluated together to approximate the irradiated modulus at elevated temperatures. The same decrease ratio with respect to the temperature was used to calculate the irradiated modulus at higher temperatures. This technique produced the following modulus model:

$$E = \begin{Bmatrix} 85.000 - 6.800 \times FD & at\ 21°C \\ 60.778 - 4.862 \times FD & at\ 200°C \\ 54.050 - 4.324 \times FD & at\ 250°C \\ 40.593 - 3.247 \times FD & at\ 350°C \\ 33.865 - 2.709 \times FD & at\ 400°C \\ 27.137 - 2.171 \times FD & at\ 450°C \\ 13.680 - 1.094 \times FD & at\ 550°C \end{Bmatrix} \quad (7)$$

where FD is the fission density in 10^{21} fissions/cm^3 (FD>0) and E is the irradiated modulus in GPa. In the model, the data needed for higher fission densities (>6.3×10^{21} fissions/cm^3) - existing outside the range of the original data at room temperature - were forecast via extrapolation.

Poisson's ratios of 0.32–0.41 can be found in the literature. Given the lack of details on how historical measurements were made, the Poisson's ratio was taken to be $\nu = 0.41$. This value was based on measurements made by using ultrasonic methods and is considered more reliable. Further details are found in [8].

For plastic behavior, a linear model as a function of temperature was created. The model is based on data given by Schulthess [6]:

$$\sigma_y = 1027 - 1.48 \times T \quad (8)$$

In the model, σ_y is the yield strength of unirradiated U-10Mo in MPa and T (°C) is the temperature. The relation is valid for temperatures of 21–550°C.

For the irradiated strength of U-10Mo, although bend strength data were reported by Schulthess [7], those data should not be confused with yield strength and ultimate strength, which are typically determined through tensile testing. The bend strength data reported by Schulthess [7] do, however, provide a good indication of the relative strength and loss of fuel ductility with increasing burnup.

The thermal expansion was based on data reported by Burkes [9].

TABLE 1: MEAN COEFFICIENT OF THERMAL EXPANSION

Temperature (°C)	CTE [1/°C]
21-100	11.8×10^{-6}
21-200	12.6×10^{-6}
21-300	14.1×10^{-6}
21-400	16.1×10^{-6}
21-500	16.4×10^{-6}
21-600	16.6×10^{-6}
21-700	16.7×10^{-6}
21-800	17.2×10^{-6}

The conductivity model was created as a quadratic regression of the data given in the Preliminary Qualification Report [8]:

$$k = \begin{Bmatrix} 0.0962\times FD^2 - 1.3343\times FD + 13.4 \ , at \ \ 50\ ^\circ C \\ 0.1156\times FD^2 - 1.6547\times FD + 15.6 \ , at\ 100\ ^\circ C \\ 0.1406\times FD^2 - 2.0182\times FD + 17.8 \ , at\ 150\ ^\circ C \\ 0.1725\times FD^2 - 2.4184\times FD + 20.0 \ , at\ 200\ ^\circ C \\ 0.1977\times FD^2 - 2.7449\times FD + 22.0 \ , at\ 250\ ^\circ C \\ 0.2042\times FD^2 - 2.9329\times FD + 23.9 \ , at\ 300\ ^\circ C \\ 0.1782\times FD^2 - 2.9036\times FD + 25.5 \ , at\ 350\ ^\circ C \end{Bmatrix} \quad (9)$$

In the model, k is thermal conductivity of the fuel (W/m-°C) and FD is the fission density in $\times10^{21}$ fission/cm^3. The conductivity model is valid for $0 \le FD \le 8\times10^{21}$ fission/cm^3. Model gives the conductivity of unirradiated fuel if fission density is set to zero (FD=0). It is important to note that this model was developed by using the best available data at the time. Since this work, new measurements were made, and new data have become available. So, different conductivity models that might produce different degradation results can be found elsewhere.

The model for specific heat capacity for *unirradiated* fuel material was based on a correlation proposed by Burkes [9]:

$$\mathrm{Cp} = (0.113 \times 10^3 \pm 4.28) + (7.05 \times 10^{-2} \pm 5.20 \times 10^{-3}) \cdot T \quad (10)$$

where Cp is the specific heat capacity in J/kg-K, and T is the temperature in Kelvin. The relation is valid for 300–1100 K.

The model for the specific heat capacity of *irradiated* fuel was based on data reported by Burkes [10]:

$$Cp = \begin{Bmatrix} 0.0078\times FD \ + \ 0.136 \ , \quad at\ 50\ ^\circ C \\ 0.0069\times FD \ + \ 0.139 \ , \ at\ 100\ ^\circ C \\ 0.0065\times FD \ + \ 0.143 \ , \ at\ 150^\circ C \\ 0.0068\times FD \ + \ 0.146 \ , \ at\ 200^\circ C \\ 0.0069\times FD \ + \ 0.150 \ , \ at\ 250^\circ C \\ 0.0067\times FD \ + \ 0.153 \ , \ at\ 300^\circ C \\ 0.0056\times FD \ + \ 0.157 \ , \ at\ 350^\circ C \end{Bmatrix} \quad (11)$$

where C_p is the specific heat (J/g-K) and FD is the fission density in $\times10^{21}$ fission/cm^3. The valid range for the conductivity model is $0 \le FD \le 8\times10^{21}$ fission/cm^3.

The density degradation model was developed using unirradiated density data and the fuel swelling correlation. For the unirradiated density of U-10Mo, data reported by Klein [11] were used. The irradiated density was estimated via the volume change of the fuel. In particular, the new volume at a specific fission density was calculated using the swelling correlation, and the density of irradiated fuel was estimated based on the new volume. This scheme gave the density model seen in TABLE 2.

2.5.2 Cladding behavioral models

Cladding material in this study is Al-based alloy AA6061. As-received aluminum is in -T6 temper. However, the Hot Isostatic Pressing (HIP) process effectively anneals the material, resulting in properties like those of Al6061-O, on which the cladding properties in this work are based. The available data indicate that cladding hardening would occur, and the properties become somewhat like those in Al6061-T4, at around 1.5×10^{25} n/m^2 [12].

Because of a high non-linearity in the material properties during irradiation, the physical, thermal, and mechanical properties of aluminum were implemented as functions of irradiation exposure and temperature whenever the property data were available. Behavioral models for the cladding include elasticity, plasticity, thermal expansion, neutron hardening, thermal creep (in fabrication only), and swelling. All the properties are based on temperature- and fluence-dependent data.

TABLE 2: DENSITY DEGRADATION MODEL

FD ($\times10^{21}$ fis/cm^3)	0.00	1.00	2.00	3.00	4.00	5.00	6.00	7.00	8.00
Temperature [°C]	By Klein	Irradiated density, estimated based on total swelling of the fuel [kg/m^3]							
20	17130	16375	15509	14577	13616	12658	11727	10839	10004
100	17060	16308	15446	14517	13560	12607	11679	10795	9963
200	16970	16222	15364	14440	13489	12540	11618	10738	9910
300	16880	16136	15283	14364	13417	12474	11556	10681	9858
400	16800	16059	15210	14296	13354	12415	11501	10630	9811
500	16710	15973	15129	14219	13282	12348	11440	10573	9759
550	16660	15925	15083	14177	13242	12311	11406	10542	9729
600	16620	15887	15047	14143	13211	12281	11378	10516	9706
700	16530	15801	14966	14066	13139	12215	11317	10460	9654

Additional details on the behavioral models of the cladding material, the literature review, and the critical assessment of the available material property data are given elsewhere [8].

2.5.3 Diffusion barrier behavioral models

The diffusion barrier is ASM Grade 702 commercially pure zirconium, on which the material properties referenced in this work are based. The thermal and mechanical models are based on the available temperature- and flux-dependent data, including density, specific heat, conductivity, thermal expansion, modulus, yield stress, ultimate strength, and thermal creep. Pure zirconium does not swell at fluences of up to 1×10^{26} n/m^2 at 300°C and ion doses up to 80 dpa in the temperature range of 300–600°C. Consequently, the irradiation swelling of Zr was assumed negligible.

Additional details on the behavioral model of the diffusion barrier, the in-depth literature review, and the critical assessment of the available material property data are given elsewhere [8].

2.5.4 Coolant channel model

Heat transfer between the plate surface and the reactor coolant was handled by defining a film condition on the surface. Reported coolant channel temperatures and heat transfer coefficients estimated via the Petukhov correlation were used to create this surface film condition. The same film condition was assigned to the large surfaces of the plates to avoid non-linearities.

Coolant channel temperature profiles were sampled from the MP-1 experiments. Thermal analysis shows a slight increase in coolant temperature as the coolant travels through the channel. However, coolant temperatures were assumed to be constant (~65 C) along the length of the plate to eliminate possible non-linearities.

The thermo-physical properties of the coolant water were obtained from the dataset reported by Lemmon [13]. Mathematical relations were created for the coolant at 2.5 MPa, which is the nominal operating pressure of the Advanced Test Reactor. Further details on behavioral models, including coolant velocities, channel dimensions, and calculated heat transfer coefficients, are given elsewhere [14].

3. RESULTS AND DISCUSSIONS

In the base model and associated sensitivity studies, both the thermal and mechanical performances were evaluated. The purpose of the thermal analysis was to estimate fuel temperatures while demonstrating that the fuel would operate without blistering or oxide spallation. In the thermal analysis, the plates were evaluated in terms of both the blistering criteria and the

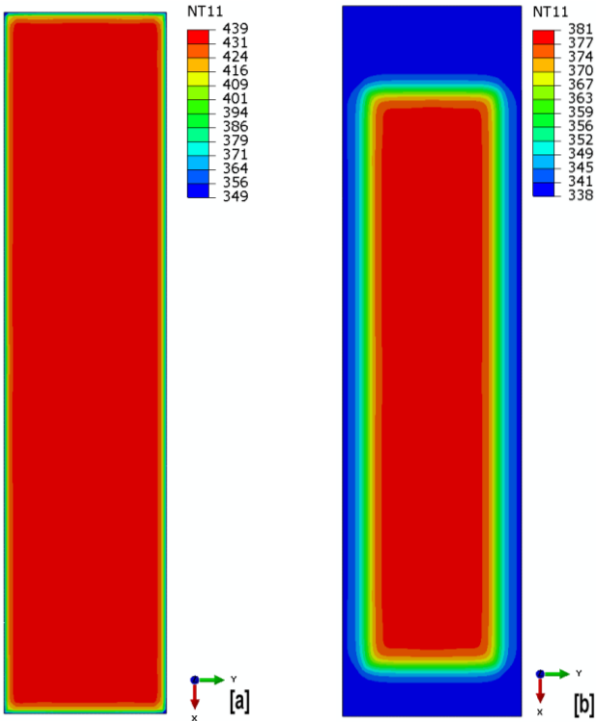

FIGURE 3: EOL TEMPERATURES (K) AT **(A)** THE FUEL MIDPLANE **(B)** THE CLADDING SURFACE

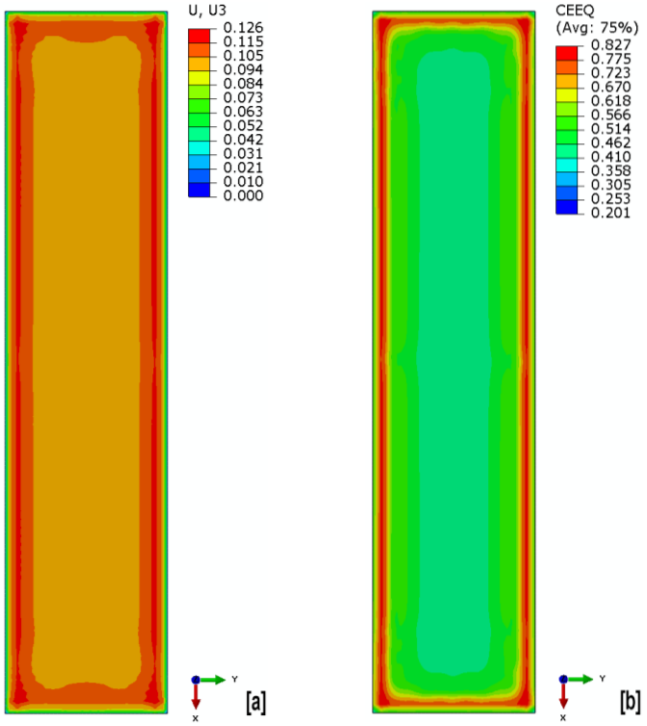

FIGURE 4: FUEL AT SHUTDOWN **(A)** THICKNESS INCREASE (MM), FROM MID-PLANE; **(B)** EQUIVALENT CREEP STRAIN

oxide spallation threshold. The fuel blistering criteria show that the fuel temperature should not exceed 360°C during a condition 2 flow coast down event. The oxide spallation threshold is 119 Δ°C across the oxide layer.

Estimated temperatures are shown in FIGURE 3. Thermal and mechanical calculations are fully coupled to include non-linear geometric variations, such as thickness increase (FIGURE 4a) due to swelling and relocation of the fuel material due to irradiation induced creep (FIGURE 4b).

The temperatures are shown for EOL, just before reactor shutdown. Per the contour plots, the peak temperatures are 439 K (~166°C) at the fuel centerline, and 381 K (~108°C) at the cladding surface. These temperatures are below the blister threshold criteria. The results also indicate that the temperature difference at the oxide layer surfaces would be below the oxide spallation threshold. The results imply no issues during normal those operational conditions.

The purpose of the structural analysis was to verify that the mechanical integrity and structural stability of the plates are preserved. To ensure acceptable performance, several output variables were evaluated. The stresses and strains were checked to evaluate mechanically driven failures and possible failure modes. Large tensile stresses accompanied by sufficient material degradation could facilitate failures at shutdown, such as fuel pillowing, fracture, or delamination. These stresses and strains were estimated via simulations, and their magnitudes were then compared against the strength of the materials. Porosity interconnection was checked for possible onset of breakaway swelling. The total deformations were also evaluated to verify that structural stability has been maintained.

FIGURE 4 shows the calculated thickness increase and estimated material relocation due to irradiation creep. Deformations were generally evaluated to check for excessive channel restriction or a closure. In FIGURE 4a, the peak displacements were estimated to be 0.252 mm (0.126 mm from the mid-plane). The peaks are seen around the perimeter of the fuel, indicating plate bulging. Because the initial fuel thickness was given as 0.216 mm, a 0.252 mm change in thickness would correspond to a roughly 120% increase in thickness at these bulged regions. The initial channel thicknesses were 1.905 mm for the outer channels (Channels 1 and 5) and 2.540 mm for the inner channels (Channels 2, 3, and 4). Based on the deformations calculated, no channel blockage should occur under nominal operational conditions. Nevertheless, the calculated deformation magnitudes indicate estimate a roughly 10% reduction of the channel gap. As expected, the peak irradiation creep (FIGURE 4b) was observed at the bulged areas around the perimeter of the fuel core, at magnitudes of over 80%.

FIGURE 5 shows the fuel stresses and their evolution during different stages of the plate's lifecycle. Fabrication simulations showed that the fuel stresses due to HIP cooling could reach 350 MPa (FIGURE 5a). However, those residual stresses become somewhat unimportant, as any post-fabrication stresses in the fuel core would be relieved relatively quickly in the reactor. The results showed that, within several hours of irradiation, the fuel

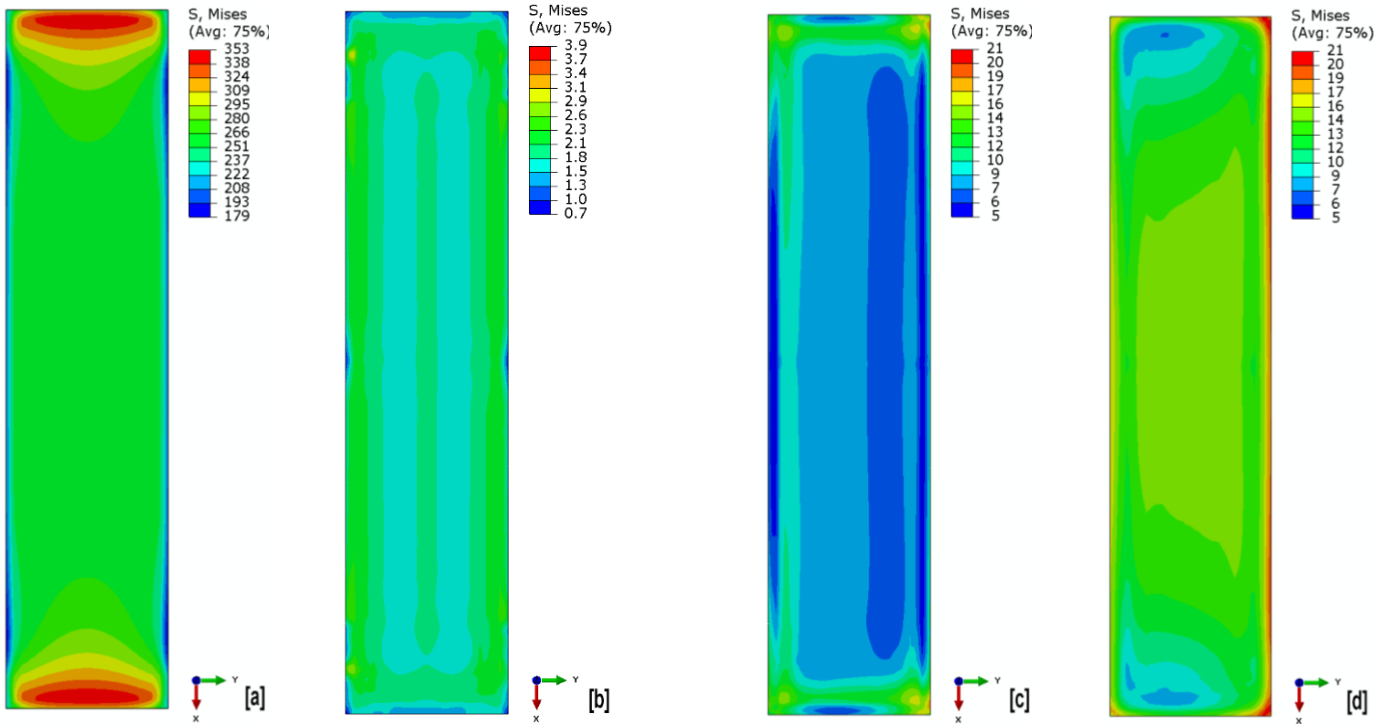

FIGURE 5: EQUIVALENT STRESSES (MPA) IN THE FUEL. CONTOURS SHOW: **(A)** END OF HIP COOLING; **(B)** IN-REACTOR, AT EOL; **(C)** AT SHUTDOWN, MIDPLANE; **(D)** AT SHUTDOWN, FUEL-DIFFUSION BARRIER INTERFACE

stresses would become negligible, and the material would be essentially stress-free during irradiation (FIGURE 5b). However, the stresses in the fuel core would develop at reactor shutdown (FIGURE 5c and FIGURE 5d).

It is important to note that this finding does not imply that all fuel elements would be stress-free in the reactor. The simulations revealed that the cladding, diffusion barrier, and interfaces would remain under stress throughout the entire irradiation period. Those irradiation stresses, especially in the cladding, increase with added exposure to neutron fluence.

Cladding stresses are shown in FIGURE 6. Unlike with the fuel material, the stresses in the cladding will increase during irradiation. Peak stresses due to HIP were calculated to be 68 MPa in the cladding (FIGURE 6a). These stresses increase to approximately 130 MPa in the reactor at EOL, roughly doubling in magnitude (FIGURE 6b). This increase is primarily due to irradiation hardening. The additional stresses in the cladding are due to straining caused by the fuel core swelling.

Stresses in the diffusion barrier are shown in FIGURE 7. Fabrication simulations (FIGURE 7a) estimated residual stresses of 316–328 MPa. Closer examination reveals that the residual stresses in the diffusion barrier would be roughly constant, apart from the isolated zones. In the reactor (FIGURE 7b), these stresses evolve substantially. Although the magnitude of the peak stresses is roughly the same, there seems to be a slight stress relief in areas closer to the center of the diffusion barrier. The peak stresses still reach around 325 MPa and appear the entire perimeter of the diffusion barrier. The magnitudes estimated by the simulations are believed to be below the strength of co-rolled, HIP processed, and irradiated pure zirconium. If so, observation of stress-driven failures in the diffusion barrier is unlikely.

4. CONCLUSION

As a supplement to the information obtained from irradiation testing, parametric sensitivity studies were extensively employed to evaluate plate performance under various input settings. To establish a reference state for those studies, a base model with a representative geometry and irradiation conditions was created. This draft introduced the base model used in those parametric sensitivity studies. The geometric features, discretization, thermal and structural coupling, material properties, behavioral models, modeling considerations, and results were all presented.

The model and the results outlined in this draft essentially lay the foundation and serve as a reference state for subsequent parametric sensitivity studies. More specifically, the selected parameters of the base model in this work varied in terms of bounding values to better elucidate irradiation performance while also evaluating the sensitivity of the performance to the various input parameters. The sensitivity studies considered various input variables, including (1) geometric, (2) operational, and (3) material-property-related parameters.

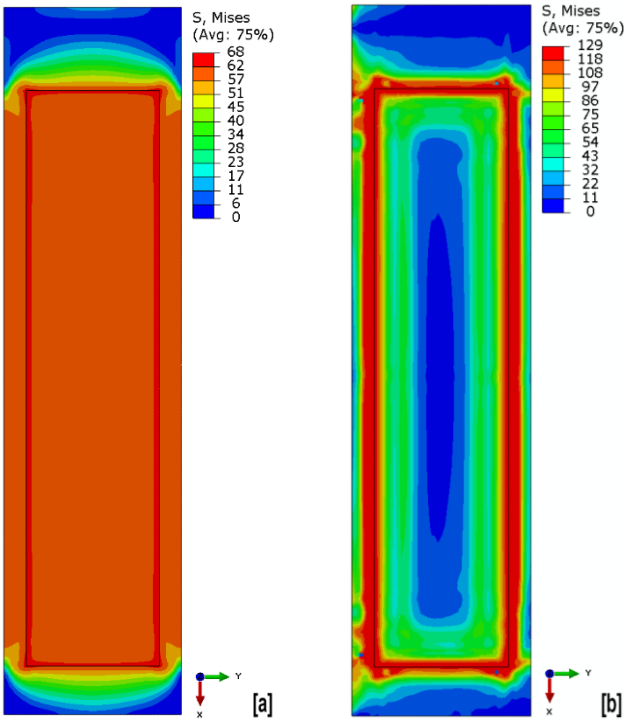

FIGURE 6: EQUIVALENT STRESSES (MPA) IN THE CLADDING: **(A)** FABRICATED, POST HIP COOLING; **(B)** IN-REACTOR, AT SHUTDOWN

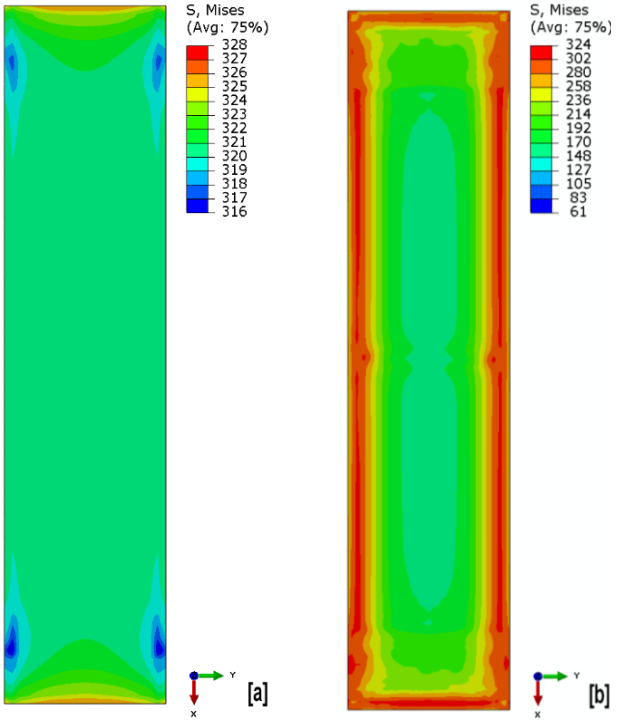

FIGURE 7: EQUIVALENT STRESSES (MPA) IN THE DIFFUSION BARRIER: **(A)** FABRICATED, POST HIP COOLING; **(B)** IN-REACTOR, AT SHUTDOWN

Sensitivity studies conducted on geometric parameters evaluated the plate performance in light of different plate geometries. In the sensitivity studies, the geometry of the base model was varied in terms of the bounding values. Those geometric parameters were (1) foil flatness, (2) diffusion barrier thickness, (3) foil corner shapes, (4) size effects, (5) plate curvature, (6) fuel thickness, (7) foil centering, (8) foil tilting, (9) burred foil, and (10) foil waviness. The key findings of the "Effects of Geometric Parameters" study are given elsewhere [15].

Sensitivity studies conducted on the operational parameters evaluated the effects of various irradiation settings on plate performance. In this regard, the base model's irradiation parameters, as summarized in this paper, were varied in terms of the bounding values. These operational parameters were (1) mechanical constraints, (2) fission profile, (3) cooling rate, (4) cooling conditions, (5) power and burnup, (6) bond strength and delamination, (7) thermal cycling, (8) residual stress state, (9) fission rate, and (10) flow-induced deformation. The key findings of the "Effects of Operational Parameters" study are given elsewhere [16].

Sensitivity studies on property-related parameters evaluated the potential effects of uncertainties in material properties and behavioral models on the simulated thermo-mechanical behavior of the fuel system. The property-related parameters were (1) diffusion barrier properties, (2) cladding properties, (3) fuel properties, (4) fuel swelling correlation, (5) fuel irradiation creep models, (6) mechanical degradation models of U-Mo, (7) thermo-physical degradation models of U-Mo, (8) oxide layer properties, (9) effects of temperature, and (10) effects of uncertainties. The key findings of the "Effects of Property Related Parameters" study are given elsewhere [17].

Documentation of the results from those sensitivity studies, along with in-depth technical evaluations, is currently underway. The results from those studies are expected to provide a better understanding of U-10Mo fuel system performance.

The authors wish to emphasize that a literature review has obtained available data and led to plans for additional measurements that may provide confidence that parametric studies undertaken will remain representative of the simulated thermo-mechanical behavior of the monolithic fuel plate. It is important to note that the material properties and behavioral models are constantly evolving as the fuel qualification program makes new property measurements. Readers are advised to obtain the latest material properties and behavioral models from the fuel qualification program to foster high-fidelity performance assessments.

ACKNOWLEDGMENTS

This work was supported by the U.S. Department of Energy, Office of Material Management and Minimization, National Nuclear Security Administration, under DOE-NE Idaho Operations Office, contract DE-AC07-05ID14517. This manuscript was authored by a contractor for the U.S. Government. The publisher, by accepting the article for publication, acknowledges that the U.S. Government retains a nonexclusive, paid-up, irrevocable, worldwide license to publish or reproduce the published form of this manuscript, or allow others to do so, for U.S. Government purposes.

REFERENCES

[1] ABAQUS, Abaqus Analysis User's Manual, Version 6.14., Providence, RI, USA: Dassault Systemes Simulia, Inc, 2014.

[2] H. Ozaltun, H. Shen and P. Medvedev, "Computational evaluation for the mechanical behavior of U10Mo fuel mini plates subject to thermal cycling," *Nuclear Engineering and Design,* vol. 254, pp. 165-178, 2013.

[3] A. Robinson, W. Williams, W. Hanson, B. Rabin, N. Lybeck and M. Meyer, "Swelling of U-Mo Monolithic Fuel: Developing a Predictive Swelling Correlation under Research Reactor Conditions," *Journal of Nuclear Materials,* vol. 544, p. 152703, 2021.

[4] Y. S. Kim and G. L. Hofman, "Fission product induced swelling of U–Mo alloy fuel," *Journal of Nuclear Materials,* vol. 419, pp. 291-301, 2011.

[5] Y. S. Kim, G. L. Hofman, J. S. Cheon, A. B. Robinson and D. M. Wachs, "Fission induced swelling and creep of U–Mo alloy fuel," *Journal of Nuclear Materials,* vol. 437, pp. 37-46, 2013.

[6] J. Schulthess, R. Lloyd, B. Rabin, M. Heighes, T. Trowbridge and E. Perez, "Elevated temperature tensile tests on DU–10Mo rolled foils," *Journal of Nuclear Materials,* vol. 510, pp. 282-296, 2018.

[7] J. Schulthess, W. Lloyd, B. Rabin, K. Wheeler and T. Walters, "Mechanical properties of irradiated U-Mo alloy fuel," *Journal of Nuclear Materials,* vol. 515, pp. 91-106, 2019.

[8] Rabin B. et.al., "INL EXT 17-40975: Preliminary Report on U Mo Monolithic Fuel for Research Reactors, Rev.04," Idaho National Laboratory, Idaho Falls, 2020.

[9] D. E. Burkes, C. Papesch, A. Maddison, T. Hartmann and F. Rice, "Thermo-physical properties of DU–10 wt. % Mo alloys," *Journal of Nuclear Materials,* vol. 403, pp. 160-166, 2010.

[10] D. Burkes, D. et.al., "Thermal properties of U-Mo alloys irradiated under high fission power density," *Journal of Nuclear Materials,* vol. 547, 2021.

[11] J. L. Klein, "Uranium and Its Alloys," in *Nuclear Reactor Fuel Elements, Ed. A.R. Kaufmann*, New York, Wiley, 1962, pp. 31, Chapter 3.

[12] K. Farrell and R. King, "Tensile Properties of Neutron-Irradiated 6061 Aluminum Alloy in Annealed and

Precipitation-Hardened Conditions," *ASTM special technical publications,* pp. 440-449, 1979.

[13] E. W. Lemmon, M. L. Huber and M. O. McLinden, "NIST Standard Reference Database 23: Reference Fluid Thermodynamic and Transport Properties - REFPROP, Version 9.1," National Institute of Standards and Technology, Gaithersburg, MD, 2013.

[14] H. Ozaltun and B. Rabin, "NUCLRF2017-3271: Thermo-mechanical performance assessment of selected plates from MP-1 high power experiments.," in *ASME 2017 Nuclear Forum collocated with the ASME 2017 Power Conference*, Charlotte, North Carolina, 2017.

[15] H. Ozaltun, H. S. Roh and W. Mohamed, "Summary of Geometric Parameters and Their Effects on Performance of U-10mo Fuel Plates," in *ASME 2022, 29th International Conference on Nuclear Engineering (ICONE29)*, Shenzhen, China, 2022.

[16] H. S. Roh, W. Mohamed and H. Ozaltun, "Effect of Operational Parameters and Their Effects on the Simulated Thermo-Mechanical Behavior of U-10Mo," in *ASME 2022 Power Conference*, Pittsburgh, PA, 2022.

[17] W. Mohamed, H. Ozaltun and H. Roh, "POWER2022-86012: Summary of Property-Related Parameters and Its Effect on the Simulated Thermo-Mechanical Behavior of U-10Mo," in *ASME 2022 Power Conference*, Pittsburgh, PA, 2022.